Rate Adaptation, Scheduling, and Mode Selection in D2D Systems with Partial Channel Knowledge

Saikiran Bulusu, *Student Member, IEEE*, Neelesh B. Mehta, *Senior Member, IEEE*, and Suresh Kalyanasundaram, *Member, IEEE*

Abstract—Device-to-device (D2D) communication enables simultaneous data transmissions by cellular users (CU) and D2D user pairs, but at the expense of additional interference between them. The literature on resource allocation in D2D systems often assumes that the base station (BS) has complete channel state information (CSI) about all the links between all the users in a cell. However, acquiring the CSI of cross links between the CUs and the D2D receivers is a critical bottleneck because the number of cross links is the product of the number of CUs and D2D pairs. We study a novel partial CSI model in which the overhead of feeding back the CSI of the cross links is much lower. For a cell with one D2D pair and multiple CUs, we propose a novel throughput-optimal joint mode selection, user scheduling, and rate adaptation policy that exploits information about the statistics of the cross links and incorporates inter-cell interference. We derive closed-form expressions for the feedback-conditioned goodput for the underlay mode, which drives this optimal policy. We also present extensions that incorporate user fairness, quantized CSI, and multiple D2D pairs and multiple subchannels.

Index Terms—D2D, Mode selection, CSI, Interference, Scheduling, Discrete rate adaptation, Feedback, Fairness.

I. INTRODUCTION

Device-to-device (D2D) communication is a promising solution for next generation cellular systems, in which D2D users (DUs) share the available spectrum with the cellular users (CUs) under the control of the base station (BS). The DUs can communicate with each other directly, which reduces the traffic load on the BS, improves frequency reuse and cell throughput, and reduces latency [1]–[3].

Given a set of user equipments (UEs) in a cellular system, some of which are D2D pairs and the rest are CUs, the problem of joint mode selection, user scheduling, and rate adaptation arises. Mode selection determines whether a subchannel should be allocated to only a D2D pair, which is called dedicated mode (DM); to only a CU, which is called cellular mode CM); or to both together, which is called underlay mode (UM). While two data transmissions

happen simultaneously in UM, they interfere with each other. User scheduling determines which CU or D2D pair or both should be allocated the subchannel based on the mode of operation. Lastly, rate adaptation determines the data rates of the scheduled CU and/or the D2D pair.

A. Related Literature

Various approaches have been pursued in the D2D literature to address some or all of the above three inter-connected problems. These differ depending on whether continuous or discrete rate adaptation is assumed. In continuous rate adaptation, the rate is assumed to take any positive real value with the Shannon capacity formula typically being used to map the signal-to-noise ratio (SNR) or signal-to-interference-plus-noise ratio (SINR) to the rate. Instead, in discrete rate adaptation, which is used in practice, a modulation and coding scheme (MCS) is selected from a pre-specified set.

Continuous Rate Adaptation: In [1], [4], for UM, the BS associates a D2D pair with a CU that causes least interference to the D2D receiver (DRx). Instead, in [5], power control at the D2D transmitter (DTx) is employed to control the interference it causes to the CU. In [2], [6], for UM, transmit power allocation strategies for one CU and one or multiple D2D pairs are proposed. This approach is extended to also consider CM and DM for single and multi-cell scenarios with co-channel interference in [3], [7]. In [8], UM is used if the average SNR at the DRx exceeds a threshold. Else, DM is used. In [9]–[11], multiple D2D pairs are allowed to reuse the radio resource of one CU, unlike the models in [1]–[8]. In [12], a scheduling algorithm for UM that ensures fairness and determines whether two devices should directly communicate with each other or via the BS is proposed. In [13], the effect of multiple antennas and inter-cell interference (ICI) on the spectral efficiency of UM is studied using stochastic geometry.

Discrete Rate Adaptation: In [14], the CUs are first allocated subchannels and their rates are selected subject to a peak power constraint. Among the available D2D pairs, the one that maximizes the sum rate subject to a minimum rate constraint for the CU is selected. In [15], the sum throughput of the D2D pairs is maximized subject to a CU rate constraint using a conflict graph approach.

B. Problem Motivation, Focus, and Contributions

A critical and common assumption in [2]–[4], [6], [8], [9], [11], [14] is that complete instantaneous channel state information (CSI) of the CU-BS links, D2D pair links, and

DTx-BS links, which we shall refer to as *direct links*, and of the CU-DRx links, which we shall refer to as *cross links*, is available at the BS.

However, the overheads incurred in acquiring the CSI of the direct links and cross links are fundamentally different. Specifically, in a cell with N CUs and M D2D pairs, the BS needs to know the CSI of M D2D pair links, M DTx-BS links, N CU-BS links, and NM CU-DRx links. In the uplink frequency or uplink subframes, in which D2D communication is preferred, the BS can itself acquire the CSI of the N CU-BS links and the M DTx-BS links by listening to transmissions by the CUs and DTxs with no additional overhead. Since the CSI of the M D2D pair links is not available at the BS, it has to be fed back to it by DRx of the D2D pair. Thus, the overhead of feeding back the CSI of the direct links scales as $O(M)$.

The CSI of the NM cross links between the CUs and the DRxs is also not available at the BS. Only a DRx can estimate the CSI of the links from N CUs to it by overhearing their data or sounding reference signal transmissions [16, Ch. 15.6], and can feed it back to the BS. The total overhead of doing so in a cell is $O(MN)$, which is much larger than that for the direct links. Ensuring timely feedback of all this CSI is very challenging [16, Ch. 10], [17]–[20].

Methods that reduce the cross-link feedback overhead in D2D systems, which is a critical bottleneck, optimal resource allocation by the BS when it has partial CSI, and an evaluation of their effectiveness are the focus of this paper. We make the following contributions:

- For a cellular system with multiple CUs and a D2D pair, we derive from first principles a novel cross-link inter-ference statistics-aware adaptation scheme (CLISAA). It specifies the throughput-optimal mode selection, schedul-ing, and rate for a given subchannel for a practically well-motivated feedback model in which the BS has at most one bit of feedback about each CU-DRx cross link. This then serves as a foundation for subsequent practically motivated extensions to the orthogonal frequency division multiplexing (OFDM) scenario with multiple subchan-nels, CUs, and D2D pairs, and when the BS has quantized CSI about the direct link between the DTx and DRx.

- For discrete rate adaptation, we show that for UM, CLISAA is driven by the feedback-conditioned goodput of each MCS. It is the product of the rate of the MCS and the probability that it can be decoded by the receiver conditioned on the CSI fed back.

- We derive closed-form expressions for the feedback-conditioned goodput for each mode and MCS. This is done for the *distance-aware scenario*, in which the BS knows the distance between the CU and the DRx, and the *distance-unaware scenario*, in which the BS does not know the above distance. The latter is practically well motivated since the locations of the UEs are often available only coarsely at the BS.

- We also extend CLISAA to ensure fairness across the UEs. We show that it achieves a higher geometric mean (GM) of the average rates of the UEs than the other benchmark schemes. GM is a widely used performance

measure in cellular system design because it takes both throughput and fairness of all the UEs into considera-tion [21], [22].

Differences with Literature: We do not assume complete CSI at the BS unlike [2]–[4], [6], [8], [9], [11], [14]. Secondly, unlike [23]–[26] which focus only on UM, we consider joint mode selection, scheduling, and rate adaptation, which leads to a different problem formulation and solution. Moreover, unlike [1]–[4], [6]–[9], [23], [24], we study discrete rate adaptation. It is practically important but has been relatively less investigated for D2D systems, and leads to a novel solution and insights. Maximizing the ergodic capacity gain, which is studied in [23]–[26], requires channel coding over many channel fades in practice. This is not required by our approach. Furthermore, [8], [9], [27] assume a fixed distance between a DTx and DRx. However, in practice, this distance is random since the user locations are random and since D2D pairing is likely to be driven by a commonality of user interests in addition to proximity. We instead allow for any two UEs in the cell to become a D2D pair and capture the randomness in the distance between them; this affects mode selection, scheduling, and rate adaptation. Lastly, we also incorporate fairness, unlike the above references. While [28] considers proportional fair scheduling, complete CSI is assumed to be fed back to the BS and only UM is considered.

C. Outline and Notation

The system model and problem statement are presented in Section II. The proposed scheme is developed in Section III. Its extensions that incorporate fairness, quantized direct-link CSI, and multiple D2D pairs are presented in Section IV. Numerical results are presented in Section V, and are followed by our conclusions in Section VI.

Notation: The probability of an event A and the conditional probability of A given B are denoted by $\Pr(A)$ and $\Pr(A|B)$, respectively. The expectation with respect to a random variable (RV) X is denoted by $\mathbb{E}_X[.]$. The indicator function $1_{\{z\}}$ is 1 if z is true and is 0 otherwise. The function $[x]^+$ denotes $\max\{x, 0\}$, $\Gamma(a)$ denotes the gamma function, and $\gamma(a, x)$ denotes the lower incomplete gamma function [29].

II. SYSTEM MODEL AND PROBLEM STATEMENT

The system model is illustrated in Fig. 1. It comprises of a circular cell of radius R, within which are N CUs indexed $1, 2, \ldots, N$ and M D2D pairs indexed $1, 2, \ldots, M$. The BS needs to determine which CU and/or D2D pair to schedule on a given subchannel and their MCSs. We focus on the uplink since it avoids the larger cross-link interference from the BSs [1], [2].

A. Channel Model

The channel gain q_{ij} between CU i and the DRx of D2D pair j is given as per the simplified path-loss model [30, Ch. 2] by

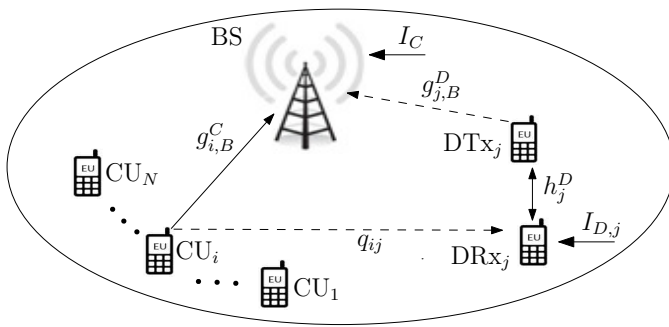$$q_{ij} = K\beta_{ij}d_{ij}^{-\alpha}, \tag{1}$$

Fig. 1. System model illustrating the BS, N CUs, and one D2D pair with one transmitter and one receiver.

where K is a path-loss constant, α is the path-loss exponent, and β_{ij} is a unit power Nakagami-m RV with parameter m that models small-scale fading, and d_{ij} is the distance between CU i and the DRx of the D2D pair j.

Similarly, let the channel gain between the DTx and DRx of D2D pair j be denoted by h_j^D and the distance between them by d_j^D. The channel gain between CU i and the BS is denoted by $g_{i,B}^C$, and that between the DTx of D2D pair j and the BS by $g_{j,B}^D$. Let $\mathbf{g}_B^C = (g_{1,B}^C, g_{2,B}^C, \ldots, g_{N,B}^C)$. The corresponding distance between CU i and the BS is denoted by $d_{i,B}^C$, and between the DTx of D2D pair j and the BS by $d_{j,B}^D$. The small-scale fading power gain of the link between the DTx and DRx of D2D pair j is denoted by β_j^D, between CU i and the BS by $\beta_{i,B}^C$, and between the DTx of D2D pair j and the BS by $\beta_{j,B}^D$. The additive white Gaussian noise (AWGN) at the DRx and the BS has variance σ^2.

B. Discrete Rate Adaptation Model

The BS has a set of L MCSs indexed by $1, 2, \ldots, L$ with rates $0 = r_1 < r_2 < \cdots < r_L$. A rate r_l can be successfully decoded if the SINR at the receiver exceeds a threshold λ_l. Here, $\lambda_1, \lambda_2, \ldots, \lambda_L$ are called rate adaptation thresholds and satisfy $0 = \lambda_1 < \lambda_2 < \cdots < \lambda_L < \lambda_{L+1} = \infty$. The rate r_l and threshold λ_l are related by $r_l = \log_2(1 + \eta\lambda_l)$, for $1 \le l \le L$, where η is the coding loss [31].

C. D2D Modes Description

We now characterize the resultant SINR for each mode.

1) Underlay Mode: Let D2D pair j use the same radio resource as CU i. Then, the SINR $\Gamma_i^{\text{UM}}(j)$ of the D2D pair j after accounting for the cross-link interference is given by

$$\Gamma_i^{\text{UM}}(j) = P_D h_j^D / \left(P_C q_{ij} + I_{D,j} + \sigma^2 \right), \qquad (2)$$

where P_D and P_C are the transmit powers of the DTx of D2D pair j and CU i, respectively, and $I_{D,j}$ is the ICI at the DRx. Similarly, the SINR $\gamma_j^{\text{UM}}(i)$ of CU i is given by

$$\gamma_j^{\text{UM}}(i) = P_C g_{i,B}^C / \left(P_D g_{j,B}^D + I_C + \sigma^2 \right), \qquad (3)$$

where I_C is the ICI at the BS receiver.

2) Cellular Mode: If CU i is scheduled, then its uplink SINR $\gamma^{\text{CM}}(i)$ is given by

$$\gamma^{\text{CM}}(i) = P_C g_{i,B}^C / \left(I_C + \sigma^2 \right). \qquad (4)$$

3) Dedicated Mode: In this mode, only the DTx transmits to the DRx. Hence, the SINR $\Gamma^{\text{DM}}(j)$ of D2D pair j is

$$\Gamma^{\text{DM}}(j) = P_D h_j^D / \left(I_{D,j} + \sigma^2 \right). \qquad (5)$$

Modeling of ICI: We model ICI using the concept of rise-over-thermal (RoT), which has been used widely in cellular system analysis [32, Ch. 8.2], [16, Ch. 18.3] as it is insightful. We define it as the ratio of the total received ICI power and the noise power. The greater the RoT, the more is the ICI. For ease of exposition, we shall set $(I_{D,j}/\sigma^2) = (I_C/\sigma^2) = \text{RoT}$ in the analysis that follows, with RoT serving as a system parameter.[1] The more general case in which these two ratios are different can also be easily handled.

D. CSI Model for Direct Links and Cross Links

In the uplink, the BS is the receiver. Therefore, it knows the channel gains $\mathbf{g}_B^C$ and $g_{j,B}^D$, for $1 \le j \le M$. In addition, the direct-link channel gain h_j^D is fed back to the BS by D2D pair j, which incurs an overhead of $O(M)$. The DRx can estimate it by listening to pilot transmissions by the DTx. Later, in Section IV-B, we also address the scenario where the direct link CSI is quantized. Since the BS knows $g_{i,B}^C$ and $g_{j,B}^D$, it follows from (3) that it can compute the SINR of CU i in UM, $\gamma_j^{\text{UM}}(i)$ and from (4), it can compute the SINR of CU i in CM, $\gamma^{\text{CM}}(i)$. Also, since the BS knows h_j^D, it follows from (5) that it can compute the SINR of D2D pair j in DM, $\Gamma_{\text{DM}}(j)$.

However, the BS does not know the cross-link gain q_{ij} since it is neither a transmitter nor a receiver for it. Only the D2D pair j can estimate q_{ij} by listening to the transmissions of CU i to the BS. The BS needs the gains of NM cross links to be able to compute the SINR for every combination of D2D pair and CU in UM so that it can schedule the optimal CU and D2D pair for it. Hence, the D2D pair has to feedback the cross-link CSI from each of the N CUs to the BS. The total feedback overhead is $O(NM)$. This is much more than that for the direct links.

To reduce the cross-link CSI overhead, we consider the model in which the DRx of D2D pair j feeds back only one bit $f_b(i, j)$ about q_{ij}, or equivalently $\Gamma_i^{\text{UM}}(j)$, to the BS. It is 1 if $\Gamma_i^{\text{UM}}(j) \ge \lambda_{\text{th}}$ and is 0 otherwise, where the threshold λ_{th} is a system parameter. Let $\mathbf{f}_b(j) = (f_b(1, j), f_b(2, j), \ldots, f_b(N, j))$. The scenario where the D2D pair j feeds back zero bits about the cross-link state, which is mathematically equivalent to $\lambda_{\text{th}} = 0$ or ∞ since these two settings provide no useful CSI to the BS, is a special case. We note that this model is more realistic than the complete CSI one in [2]–[4], [6], [8], [9], [11], [14].

E. Modeling Simplifications and Discussion

Our model captures several salient aspects of LTE, but not all of them. For example, it does not model hybrid automatic

---

[1]The model assumes that RoT is known to the BS, which is similar to the assumption about ICI in [13]. However, [13] does not incorporate other practical aspects such as discrete rate adaptation, variable D2D distance, quantized direct link CSI, or limited cross-link CSI.

repeat request (HARQ), single carrier frequency division multiple access (SC-FDMA), or scheduling and control channel constraints. Furthermore, we assume that the transmit powers P_C and P_D are fixed. This is justified since UL power control in LTE is primarily open loop, i.e., it compensates for pathloss but not small-scale fading because of its orthogonal channelization. Such simplifications are necessary in order to ensure that the model is analytically tractable and yields mathematically rigorous design insights. We also note that the results can be generalized to the scenario where the transmit powers of different UEs are different, which captures the above open-loop power control.

III. RATE ADAPTATION WITH PARTIAL CSI

In order to gain insights, we first consider one D2D pair j and N CUs in a cell and one subchannel to be scheduled. It serves as the foundation for understanding the multiple D2D pairs and subchannels scenario that we study next in Section IV-C. We extend it to ensure UE fairness in Section IV-A.

We set up the following notation in order to formally state the problem. Let m_1 be an indicator variable whose value is 1 if UM is selected, and is 0 otherwise. Similarly, m_2 and m_3 are the indicator variables for CM and DM, respectively. Let $\mathbf{m} = (m_1, m_2, m_3)$. In UM (or CM), let x_i^{UM} (or x_i^{CM}) be the indicator variable whose value is 1 if CU i is scheduled to use the subchannel, and is 0 otherwise. Let $\mathbf{x}^{\text{UM}} = \left(x_1^{\text{UM}}, x_2^{\text{UM}}, \ldots, x_N^{\text{UM}}\right)$ and $\mathbf{x}^{\text{CM}} = \left(x_1^{\text{CM}}, x_2^{\text{CM}}, \ldots, x_N^{\text{CM}}\right)$.

To track the MCS assigned, for UM, let $z_l^D(j, i)$ be the indicator variable whose value is 1 if MCS l is selected for rate adaptation by D2D pair j when scheduled with CU i, and let $z_l^C(i, j)$ be the indicator variable whose value is 1 if MCS l is selected for CU i. Let $\mathbf{z}^C(i, j) = \left(z_1^C(i, j), z_2^C(i, j), \ldots, z_L^C(i, j)\right)$ and $\mathbf{z}^D(j, i) = \left(z_1^D(j, i), z_2^D(j, i), \ldots, z_L^D(j, i)\right)$. Similarly, for CM, let $z_l^{\text{CM}}(i)$ be the indicator variable whose value is 1 if MCS l is selected for CU i. Let $\mathbf{z}^{\text{CM}}(i) = \left(z_1^{\text{CM}}(i), z_2^{\text{CM}}(i), \ldots, z_L^{\text{CM}}(i)\right)$. And, for DM, let $z_l^{\text{DM}}(j)$ be the indicator variable whose value is 1 if MCS l is selected by D2D pair j. Let $\mathbf{z}^{\text{DM}}(j) = \left(z_1^{\text{DM}}(j), z_2^{\text{DM}}(j), \ldots, z_L^{\text{DM}}(j)\right)$.

The instantaneous throughput T is then given by:

$$T = m_1 \left[\sum_{i=1}^{N} x_i^{\text{UM}} \left(\sum_{l=1}^{L} z_l^C(i, j) r_l 1_{\left\{\gamma_j^{\text{UM}}(i) \geq \lambda_l\right\}} \right. \right.$$
$$\left. + \sum_{l=1}^{L} z_l^D(j, i) r_l 1_{\left\{\Gamma_i^{\text{UM}}(j) > \lambda_l\right\}} \right) \Bigg]$$
$$+ m_2 \left[\sum_{i=1}^{N} x_i^{\text{CM}} \sum_{l=1}^{L} z_l^{\text{CM}}(i) r_l 1_{\left\{\gamma^{\text{CM}}(i) \geq \lambda_l\right\}} \right]$$
$$+ m_3 \left[\sum_{l=1}^{L} z_l^{\text{DM}}(j) r_l 1_{\left\{\Gamma^{\text{DM}}(j) \geq \lambda_l\right\}} \right]. \quad (6)$$

At any time instant, the problem of maximizing the fading-averaged cell throughput with one D2D pair, say j, given the

partial CSI available at the BS is as follows:

$$\max_{\substack{\mathbf{m}, \mathbf{x}^{\text{UM}}, \mathbf{x}^{\text{CM}}, \mathbf{z}^D(j,i), \\ \mathbf{z}^C(i,j), \mathbf{z}^{\text{CM}}(i), \mathbf{z}^{\text{DM}}(j)}} \mathbb{E}_{q_{ij}}\left[T | \mathbf{g}_B^C, g_{j,B}^D, h_j^D, \mathbf{f}_b(j)\right], \quad (7)$$

$$\text{s.t.} \quad \sum_{v=1}^{3} m_v = 1, \sum_{i=1}^{N} x_i^{\text{UM}} = 1, \sum_{i=1}^{N} x_i^{\text{CM}} = 1,$$

$$\sum_{l=1}^{L} z_l^D(j, i) = 1, \sum_{l=1}^{L} z_l^{\text{DM}}(j) = 1, \sum_{l=1}^{L} z_l^C(i, j) = 1,$$

$$\sum_{l=1}^{L} z_l^{\text{CM}}(i) = 1, \text{ for } 1 \leq i \leq N, \quad (8)$$

$$m_1, m_2, m_3 \in \{0, 1\}, x_i^{\text{UM}} \in \{0, 1\}, x_i^{\text{CM}} \in \{0, 1\},$$
$$z_l^D(j, i) \in \{0, 1\}, z_l^C(i, j) \in \{0, 1\}, z_l^{\text{CM}}(i) \in \{0, 1\},$$
$$z_l^{\text{DM}}(j) \in \{0, 1\}, \text{ for } 1 \leq i \leq N \text{ and } 1 \leq l \leq L. \quad (9)$$

The constraints in (8) ensure that only one mode can be selected, only one CU in UM can be scheduled, only one CU in CM can be scheduled, only one MCS for D2D pair j when scheduled with CU i in UM can be selected, only one MCS for D2D pair j in DM can be selected, only one MCS for CU i in UM can be selected, and only one MCS for CU i in CM can be selected.

Result *1:* The optimal solution of (7) consists of the following three steps:

1. Rate Selection: In this step, the rates for all the UEs are selected for each mode of operation by the BS. For UM, the optimal MCS index $l_{\text{DU}}^*(j, i)$ for D2D pair j when scheduled with CU i is

$$l_{\text{DU}}^*(j, i) =$$
$$\underset{1 \leq l \leq L}{\text{argmax}} \left\{ r_l \text{Pr}\left(\Gamma_i^{\text{UM}}(j) > \lambda_l | \mathbf{f}_b(j), \mathbf{g}_B^C, g_{j,B}^D, h_j^D\right) \right\}, \quad (10)$$

and the optimal MCS index $l_{\text{CU}}^*(i, j)$ for CU i, for $1 \leq i \leq N$, is

$$l_{\text{CU}}^*(i, j) = \underset{1 \leq l \leq L}{\text{argmax}} \left\{ r_l 1_{\left\{\gamma_j^{\text{UM}}(i) \geq \lambda_l\right\}} \right\}. \quad (11)$$

For CM, the optimal MCS index $l_{\text{CM}}^*(i)$ for CU i, for $1 \leq i \leq N$, is

$$l_{\text{CM}}^*(i) = \underset{1 \leq l \leq L}{\text{argmax}} \left\{ r_l 1_{\left\{\gamma^{\text{CM}}(i) \geq \lambda_l\right\}} \right\}. \quad (12)$$

For DM, the optimal MCS index $l_{\text{DM}}^*(j)$ for D2D pair j is

$$l_{\text{DM}}^*(j) = \underset{1 \leq l \leq L}{\text{argmax}} \left\{ r_l 1_{\left\{\Gamma^{\text{DM}}(j) \geq \lambda_l\right\}} \right\}. \quad (13)$$

2. User Scheduling and Resultant Throughput: This step specifies the CU to be scheduled for UM and CM. For UM, the CU i_{UM}^* that is scheduled is given by

$$i_{\text{UM}}^* = \underset{1 \leq i \leq N}{\text{argmax}} \left\{ r_{l_{\text{CU}}^*(i,j)} + r_{l_{\text{DU}}^*(j,i)} \right\}, \quad (14)$$

and the throughput τ_{UM} is equal to $r_{l_{\text{CU}}^*(i_{\text{UM}}^*, j)} + r_{l_{\text{DU}}^*(j, i_{\text{UM}}^*)}$. For CM, the CU i_{CM}^* that is scheduled is

$$i_{\text{CM}}^* = \underset{1 \leq i \leq N}{\text{argmax}} \left\{ r_{l_{\text{CM}}^*(i)} \right\}, \quad (15)$$

and the throughput τ_{CM} is equal to $r_{l_{\text{CM}}^*(i_{\text{CM}}^*)}$. For DM, the throughput τ_{DM} is equal to $r_{l_{\text{DM}}^*(j)}$.

3. Mode Selection: In this step, the mode of operation k^* that maximizes the cell throughput conditioned on the CSI available at the BS is selected. It is given by

$$k^* = \underset{u \in \{\text{UM,CM,DM}\}}{\text{argmax}} \{\tau_u\}. \qquad (16)$$

Proof: The proof, which follows from first principles and exploits the additive form of T, is given in Appendix A. ∎

The key notation used thus far is summarized in Table I.

TABLE I
KEY SYSTEM PARAMETERS AND VARIABLES

Description	Parameter
Cross-link channel gain between CU i and DRx of D2D pair j	q_{ij}
Distance between CU i and DRx of D2D pair j	d_{ij}
Channel gain between CU i and BS	$g_{i,B}^C$
Channel gain between DTx of D2D pair j and BS	$g_{j,B}^D$
Channel gain between DTx and DRx of D2D pair j	h_j^D
ICI at DRx of D2D pair j and at BS	$I_{D,j}$ and I_C
Rise-over-thermal	RoT
D2D pair j: SINR in UM, CM	$\Gamma_i^{\text{UM}}(j)$, $\Gamma_i^{\text{DM}}(j)$
CU i: SINR in UM, CM	$\gamma^{\text{UM}}(i)$, $\gamma^{\text{CM}}(i)$
N-bit feedback vector from D2D pair j to BS	$\mathbf{f}_b(j)$
Optimal MCS index for CU i in UM (with D2D pair j), CM	$l_{\text{CU}}^*(i,j)$, $l_{\text{CM}}^*(i)$
Optimal MCS index for D2D pair j in UM (with CU i), DM	$l_{\text{DU}}^*(j,i)$, $l_{\text{DM}}^*(j)$
CU scheduled in UM, CM	i_{UM}^*, i_{CM}^*

Computational Complexity: In (10), the feedback-conditioned goodput of a D2D pair in UM is computed by the BS for each of the N CUs it could transmit with and for the L MCSs. Closed-form expressions for it are derived below. Thus, for a D2D pair, the computational complexity of this is $O(NL)$. Similarly, the complexity for determining the optimal MCSs for the N CUs in UM and CM is $O(NL)$, and for the D2D pair in DM is $O(L)$. Therefore, the total complexity of this step is $O(NL + L)$. The complexity of the user scheduling step is $O(N)$ since it involves finding the best CU among the N CUs for both UM and CM. The complexity of the third step is $O(1)$ since it requires comparing the throughputs of the 3 modes. Therefore, the total computational complexity is $O(NL + L + N)$. This is the same as that with complete CSI.

Interpretation and Significance of Result 1: The result proves that rate selection by the optimal policy takes a mixed form. For a CU in UM and CM, and for the D2D pair in DM, it is the same as conventional rate adaptation [14], [15], in that the MCS with the highest rate for which the SINR exceeds the corresponding decoding threshold is selected. However, for a D2D pair in UM, the optimal MCS is the one that maximizes the *feedback-conditioned goodput*, which is the average number of bits that the DRx successfully decodes when the DTx transmits conditioned on the partial CSI available at the BS. This occurs since the BS does not know the D2D SINR in UM. Secondly, it is very general. It applies to both distance-aware and distance-unaware scenarios. It is novel even for the special case of no feedback for both these scenarios.

A. Distance-Aware Scenario

In this case, $Kd_{ij}^{-\alpha}$ is known to the BS. Recall that β_{ij} is a Nakagami-m RV and that in 1-bit cross-link feedback, $f_b(i,j)$ is 1 if $\Gamma_i^{\text{UM}}(j) \geq \lambda_{\text{th}}$ and is 0 otherwise.

Result *2:* For 1-bit cross-link feedback, the feedback-conditioned goodput of MCS l of D2D pair j in UM is

$$r_l \Pr\big(\Gamma_i^{\text{UM}}(j) > \lambda_l | \mathbf{f}_b(j), \mathbf{g}_B^C, g_{j,B}^D, h_j^D\big)$$
$$= \begin{cases} r_l \frac{\Psi(\max\{\lambda_l,\lambda_{\text{th}}\})}{\Psi(\lambda_{\text{th}})}, & f_b(i,j) = 1, \\ r_l - r_l \frac{\Gamma(m)-\Psi(\min\{\lambda_l,\lambda_{\text{th}}\})}{\Gamma(m)-\Psi(\lambda_{\text{th}})}, & \text{else,} \end{cases} \qquad (17)$$

where $\Psi(x) = \gamma\left(m, m\left[\frac{[P_D h_j^D - (1+\text{RoT})\sigma^2 x]^+}{P_C K d_{ij}^{-\alpha} x}\right]^2\right)$.

Proof: The proof is relegated to Appendix B. ∎

B. Distance-Unaware Scenario

In this case, d_{ij} is itself an RV that is unknown to the BS and needs to be averaged over to evaluate the optimal MCS in (10). The distance between the CU and DRx, both of which can be anywhere in the cell area, has an involved, intractable probability density function (PDF) that is given in [33, (42)]. The following bounding approach circumvents this problem.

Lemma *1:* Let d_{ij}' denote the distance between CU i and the DRx of D2D pair j when the CU is assumed to be at the cell center and the DRx is uniformly distributed in a cell of radius R. The RV d_{ij} stochastically dominates[2] the RV d_{ij}'.

Proof: The proof is given in Appendix C. ∎

From [9], the PDF of d_{ij}' is $f_{d_{ij}'}(d) = 2d/R^2$, for $0 \leq d \leq R$. Hence, the lemma implies that replacing the intractable PDF of d_{ij} with the tractable PDF of d_{ij}' leads to an underestimation of the distance and path-loss, and, thus, an underestimation of the SINR $\Gamma_i^{\text{UM}}(j)$ and the MCS $l_{\text{DU}}^*(j,i)$ that maximizes the feedback-conditioned goodput $\mathbb{E}_{d_{ij}}\big[\Pr(\Gamma_i^{\text{UM}}(j) \geq \lambda_l | \mathbf{g}_B^C, g_{j,B}^D, h_j^D, \mathbf{f}_b(j))\big]$. In the following, while averaging over the distance, we focus on Rayleigh fading ($m = 1$) in order to ensure analytical tractability.

Result *3:* Let $\zeta(\lambda) = (P_D h_j^D - (1 + \text{RoT})\sigma^2\lambda)/(P_C K\lambda)$. The feedback-conditioned goodput of MCS l of D2D pair j in UM is given as follows for $m = 1$. If $f_b(i,j) = 1$, then

$$r_l \Pr\big(\Gamma_i^{\text{UM}}(j) > \lambda_l | \mathbf{f}_b(j), \mathbf{g}_B^C, g_{j,B}^D, h_j^D\big)$$
$$\approx \frac{2r_l}{\alpha R^2} \sum_{n=1}^{\infty} \gamma\left(\frac{2}{\alpha}, \zeta(\lambda_{\text{th}})nR^\alpha\right)(\zeta(\lambda_{\text{th}})n)^{-\frac{2}{\alpha}}$$
$$- \frac{2r_l}{\alpha R^2} \sum_{n=1}^{\infty} \frac{\gamma\left(\frac{2}{\alpha}, [\zeta(\lambda_{\text{th}})n + \zeta(\max\{\lambda_l,\lambda_{\text{th}}\})]R^\alpha\right)}{(\zeta(\lambda_{\text{th}})n + \zeta(\max\{\lambda_l,\lambda_{\text{th}}\}))^{\frac{2}{\alpha}}}. \qquad (18)$$

Else,

$$r_l \Pr\big(\Gamma_i^{\text{UM}}(j) > \lambda_l | \mathbf{f}_b(j), \mathbf{g}_B^C, g_{j,B}^D, h_j^D\big)$$
$$\approx r_l - \frac{2r_l}{\alpha R^2} \frac{\gamma\left(\frac{2}{\alpha}, [\zeta(\min\{\lambda_l,\lambda_{\text{th}}\}) - \zeta(\lambda_{\text{th}})]R^\alpha\right)}{(\zeta(\min\{\lambda_l,\lambda_{\text{th}}\}) - \zeta(\lambda_{\text{th}}))^{\frac{2}{\alpha}}}. \qquad (19)$$

Proof: The proof is relegated to Appendix D. ∎

[2]An RV X with cumulative distribution function (CDF) $F_X(\cdot)$ is said to stochastically dominate an RV Y with CDF $F_Y(\cdot)$ if $F_X(x) \leq F_Y(x), \forall x$.

In both scenarios, the optimal rates for each CU in UM and CM, and for the D2D pair in DM are obtained from (11), (12), and (13), respectively. Subsequently, the user scheduling and mode selection steps occur as per (14), (15), and (16). The corresponding results for the no feedback case are obtained by substituting λ_{th} to 0 or ∞ in (17), (18), and (19). We note that even these results are novel as they exploit the statistics of cross-link interference.

IV. PRACTICALLY RELEVANT EXTENSIONS

We now present three practically relevant extensions that incorporate: (i) user fairness, (ii) use quantized direct-link CSI, and (iii) multiple D2D pairs in a cell with multiple orthogonal subchannels.

A. Incorporating Cellular and D2D User Fairness

To incorporate fairness, we introduce time t into our notation, and first define the instantaneous weighted sum throughput $T'(t)$ at time t as

$$
T'(t) = m_1 \left[\sum_{i=1}^{N} x_i^{\text{UM}} \left(w_i^C(t) \sum_{l=1}^{L} z_l^C(i,j) r_l 1_{\{\gamma_j^{\text{UM}}(i) \geq \lambda_l\}} \right. \right.
$$
$$
\left. + w_j^D(t) \sum_{l=1}^{L} z_l^D(j,i) r_l 1_{\{\Gamma_i^{\text{UM}}(j) > \lambda_l\}} \right) \Bigg]
$$
$$
+ m_2 \left[\sum_{i=1}^{N} x_i^{\text{CM}} w_i^C(t) \sum_{l=1}^{L} z_l^{\text{CM}}(i) r_l 1_{\{\gamma^{\text{CM}}(i) \geq \lambda_l\}} \right]
$$
$$
+ m_3 w_j^D(t) \left[\sum_{l=1}^{L} z_l^{\text{DM}}(j) r_l 1_{\{\Gamma^{\text{DM}}(j) \geq \lambda_l\}} \right], \quad (20)
$$

where $w_i^C(t)$ and $w_j^D(t)$ are the weights associated with CU i and D2D pair j, respectively, at time t.[3] To ensure proportional fairness, the weights are given by [34]

$$
w_i^C(t) = 1/\overline{r}_i^C(t-1) \quad \text{and} \quad w_j^D(t) = 1/\overline{r}_j^D(t-1), \quad (21)
$$

where $\overline{r}_i^C(t-1)$ and $\overline{r}_j^D(t-1)$ denote the average rates of CU i and D2D pair j until time $t-1$. A CU gets assigned a non-zero rate when it is scheduled in the UM or CM modes. And, a D2D user gets assigned a non-zero rate when it is scheduled in the UM or DM modes. Therefore, assuming that resource allocation for all the UEs starts at $t = 0$ and $\overline{r}_i^C(0) = \overline{r}_j^D(0) = 0$, these average rates are given in terms of the rates and UEs scheduled at time $(t-1)$ by

$$
\overline{r}_i^C(t-1) = \left((t-2)\overline{r}_i^C(t-2) + r_{l_{\text{CU}}^*(i,j)} 1_{\{k^*=\text{UM}\}} 1_{\{i=i_{\text{UM}}^*\}} \right.
$$
$$
\left. + r_{l_{\text{CM}}^*(i)} 1_{\{k^*=\text{CM}\}} 1_{\{i=i_{\text{CM}}^*\}} \right) / (t-1), \quad (22)
$$
$$
\overline{r}_j^D(t-1) = \left((t-2)\overline{r}_j^D(t-2) + r_{l_{\text{DU}}^*(j,i)} 1_{\{k^*=\text{UM}\}} 1_{\{i=i_{\text{UM}}^*\}} \right.
$$
$$
\left. + r_{l_{\text{DM}}^*(j)} 1_{\{k^*=\text{DM}\}} \right) / (t-1). \quad (23)
$$

[3] We do not show the dependence of the channel gains on t in order to keep the notation simple and consistent with that used earlier.

At time t, the optimal policy should maximize the following fading-averaged weighted sum throughput conditioned on the partial CSI available:

$$
\max_{\substack{\mathbf{m}, \mathbf{x}^{\text{UM}}, \mathbf{x}^{\text{CM}}, \mathbf{z}^D(j,i), \\ \mathbf{z}^C(i,j), \mathbf{z}^{\text{CM}}(i), \mathbf{z}^{\text{DM}}(j)}} \mathbb{E}_{q_{ij}} \left[T'(t) | \mathbf{g}_B^C, g_{j,B}^D, h_j^D, \mathbf{f}_b(j) \right]. \quad (24)
$$

subject to the constraints in (8) and (9). It is as follows.

Result 4: The optimal solution of (24) consists of three steps:

1. Rate Selection: This step is the same as in Result 1. The optimal MCS indices $l_{\text{DU}}^*(j,i)$ and $l_{\text{CU}}^*(i,j)$ for rate selection by the BS for the D2D pair j in UM and CU i, for $1 \leq i \leq N$, are given in (10) and (11), respectively. Similarly, the optimal MCS index $l_{\text{CM}}^*(i)$ for rate selection for CU i, for $1 \leq i \leq N$, in CM is given in (12). Furthermore, the optimal MCS index $l_{\text{DM}}^*(j)$ for rate selection for the D2D pair j in DM is given in (13).

2. User Scheduling and Resultant Weighted Sum Throughputs: For UM, the CU i_{UM}^* that is scheduled is given by

$$
i_{\text{UM}}^* = \operatorname*{argmax}_{1 \leq i \leq N} \left\{ w_i^C(t) r_{l_{\text{CU}}^*(i,j)} + w_j^D(t) r_{l_{\text{DU}}^*(j,i)} \right\}, \quad (25)
$$

and the weighted throughput τ'_{UM} is $w_{i_{\text{UM}}^*}^C(t) r_{l_{\text{CU}}^*(i_{\text{UM}}^*,j)} + w_j^D(t) r_{l_{\text{DU}}^*(j,i_{\text{UM}}^*)}$. For CM, the CU i_{CM}^* that is scheduled is

$$
i_{\text{CM}}^* = \operatorname*{argmax}_{1 \leq i \leq N} \left\{ w_i^C(t) r_{l_{\text{CM}}^*(i)} \right\}, \quad (26)
$$

and the weighted throughput τ'_{CM} is $w_{i_{\text{CM}}^*}^C(t) r_{l_{\text{CM}}^*(i_{\text{CM}}^*)}$. The weighted throughput τ'_{DM} for D2D pair j in DM is $w_j^D(t) r_{l_{\text{DM}}^*(j)}$.

3. Mode Selection: The mode of operation k^* that maximizes the weighted cell throughput is

$$
k^* = \operatorname*{argmax}_{u \in \{\text{UM,CM,DM}\}} \left\{ \tau'_u \right\}. \quad (27)
$$

Proof: $T'(t)$ has an additive form that is similar to that of T in (6) except for the weights. Hence, the proof is similar to that in Appendix A, and is skipped. ∎

B. Quantized Direct-Link CSI Feedback

With it, the BS knows the direct-link D2D SINR $P_D h_j^D / ((1+\text{RoT})\sigma^2)$ in only a quantized form as it needs to be fed back to it by D2D pair j. The quantization occurs as follows. The range of the direct-link SINR, which is $[0,\infty)$, is divided into $(L+1)$ regions $[\lambda_e, \lambda_{e+1})$, for $1 \leq e \leq L$. Index e is fed back to the BS when the SINR lies in $[\lambda_e, \lambda_{e+1})$.

For this, it can be shown that the optimal rate adaptation, mode selection, and user scheduling policy is the same as Result 1 except that the feedback-conditioned goodputs for the D2D pair j in UM and DM change as follows. For UM,

the MCS that maximizes the feedback-conditioned goodput for Nakagami-m distributed small-scale fading is given by

$$l_{\text{DU}}^*(j,i) = \operatorname*{argmax}_{1 \leq l \leq L} \left\{ r_l \Pr\left(\Gamma_i^{\text{UM}}(j) > \lambda_l | \mathbf{f}_b(j), \mathbf{g}_B^C, g_{j,B}^D, \right.\right.$$

$$\left.\left. d_{ij}, \lambda_e \leq \frac{P_D h_j^D}{(1+\text{RoT})\sigma^2} < \lambda_{e+1} \right) \right\}, \quad (28)$$

$$\approx \operatorname*{argmax}_{1 \leq l \leq L} \left\{ r_l \Pr\left(\Gamma_i^{\text{UM}}(j) > \lambda_l | \mathbf{f}_b(j), \mathbf{g}_B^C, g_{j,B}^D, \right.\right.$$

$$\left.\left. d_{ij}, P_D h_j^D = (1+\text{RoT})\sigma^2 \lambda_e \right) \right\}. \quad (29)$$

The second step follows by replacing the inequality $\lambda_e \leq P_D h_j^D / ((1+\text{RoT})\sigma^2) < \lambda_{e+1}$ with the conservative estimate of λ_e for $P_D h_j^D / ((1 + \text{RoT})\sigma^2)$. For the distance-aware scenario with Nakagami-m fading, it can be shown along lines similar to Appendix B that this simplifies as follows. For $f_b(i,j) = 1$:

$$l_{\text{DU}}^*(j,i) \approx \begin{cases} \operatorname{argmax}_{1 \leq l \leq L} \left\{ r_l \frac{\Psi'(\max\{\lambda_l, \lambda_{\text{th}}\})}{\Psi'(\lambda_{\text{th}})} \right\}, \\ \qquad\qquad\qquad\qquad\qquad f_b(i,j) = 1, \\ \operatorname{argmax}_{1 \leq l \leq L} \left\{ r_l - r_l \frac{\Gamma(m) - \Psi'(\min\{\lambda_l, \lambda_{\text{th}}\})}{\Gamma(m) - \Psi'(\lambda_{\text{th}})} \right\}, \\ \qquad\qquad\qquad\qquad\qquad \text{else}, \end{cases}$$

$$\qquad\qquad\qquad\qquad\qquad\qquad\qquad\qquad (30)$$

where $\Psi'(x) = \gamma\left(m, m\left[\frac{(1+\text{RoT})\sigma^2[\lambda_e - x]^+}{P_C K d_{ij}^{-\alpha} x}\right]^2\right)$.

The corresponding expressions for the distance-unaware scenario are not shown to conserve space. Similarly, on approximating $\Gamma^{\text{DM}}(j)$ with λ_e as above, the MCS for D2D pair j in DM is given by $l_{\text{DM}}^*(j) \approx \operatorname{argmax}_{1 \leq l \leq L} \left\{ r_l 1_{\{\lambda_e \geq \lambda_l\}} \right\}$. Fairness can also be easily incorporated along lines similar to Section IV-A.

C. Multiple D2D Pairs and Multiple Subchannels

We now consider the more general scenario where there are U subchannels per cell, N CUs, and M D2D pairs. We adopt the model in [3], in which the BS assigns a CU or a D2D pair or both to each subchannel and a D2D pair or a CU can be assigned to at most one subchannel. As before, the BS knows the channel power gains of the direct links and the feedback vector $\mathbf{f}_b(j)$, for $1 \leq j \leq M$, for each of the U subchannels.

We propose the following greedy allocation strategy that uses the insights from Result 1. The BS first calculates the rates for all UEs for all three modes for each subchannel as per (10)–(16). The subchannel with the highest sum throughput across all the three modes is first assigned. The UEs that led to this sum throughput are scheduled on this subchannel using the corresponding mode; these UEs are not considered in subsequent steps. This ensures that a CU and D2D pair is assigned to at most one subchannel, as assumed in [2], [3]. Thereafter, among the set of remaining UEs, the subchannel with the highest sum throughput across all three modes is assigned. The process continues until all the U subchannels have been assigned. Note that different subchannels can use different modes. We note that this strategy can be easily modified for the scenario where a CU can be assigned multiple subchannels.

V. SIMULATION RESULTS

We present simulation results to characterize the cell throughput with partial CSI, and gain quantitative insights into its behavior. In general, in a cell, $2M$ randomly selected UEs form M D2D pairs and the rest N UEs are CUs. The numerical results are averaged over 100 user drops. In each drop, the UE locations are randomly generated to lie with uniform probability over a circular cell of radius R, and 1000 fades of all the channels are averaged over. In each drop, the results are also averaged over all the $\binom{N+2M}{2}$ combinations of D2D pairs and, therefore, their distances. The path-loss constant K is 0.01 and path-loss exponent α is 3. The noise variance σ^2 is -114 dBm. The transmit powers of both cellular and D2D UEs are set such that the fading-averaged SNR at the BS if they are at the cell-edge is 0 dB. The coding loss factor η is 0.398 [31]. All MCSs and their rates are as specified in the channel quality indicator (CQI) feedback table of the Long Term Evolution (LTE) standard with $L = 16$ [16, Tbl. 10.1]. The rates $r_2, \ldots, r_{16}$ in this set range from 0.15 to 5.55 bits/symbol.

A. Benchmarking Schemes

We benchmark the performance of CLISAA with the following schemes.

1) Cross-link Interference Statistics Unaware Rate Adaptation (CISURA): In it, the BS does not know the cross-link gain q_{ij} to any CU, and instead uses its fading-averaged value to estimate the SINR $\Lambda_i^{\text{UM}}(j)$ at the BS as $\Lambda_i^{\text{UM}}(j) = P_D h_j^D / (P_C \mathbb{E}_{q_{ij}}[q_{ij}] + (1+\text{RoT})\sigma^2)$. Then, the MCS selected for the D2D pair j in UM when scheduled with CU i is given by $l_{\text{DU}}^*(j,i) = \operatorname{argmax}_{1 \leq l \leq L} \left\{ r_l 1_{\{\Lambda_i^{\text{UM}}(j) > \lambda_l\}} \right\}$. The rate selection for a CU in UM and CM and for a D2D pair in DM, user scheduling, and mode selection steps are similar to the proposed scheme.

2) Fixed D2D Rate (FDR): In it, the BS assumes a fixed rate r_{D2D} for the D2D pair and, thus, need not know the cross-link gain. The CU rate, user scheduling, and mode selection steps are similar to the proposed scheme. Note that depending on the SINR $\Gamma_i^{\text{UM}}(j)$, the data transmitted with this rate may not be decoded by the DRx.

3) Ideal Complete CSI Scheme: In it, the BS knows the instantaneous channel gains of all the direct links and cross links in the system [2], [3]. Using these, it performs optimal rate selection, user scheduling, and mode selection. This provides an upper limit to compare against.

B. Performance and Comparison Results

In order to characterize the impact of different system parameters, we present results for several combinations of system parameters and scenarios. Fig. 2 shows the effect of λ_{th}. Figs. 3 and 4 show benchmarking results. These figures focus on $M = 1$ D2D pair, since the optimal policy was first characterized for it. We first do this with RoT set to 0. Thereafter, the multiple D2D pairs scenario is studied in Fig. 5, which shows the effect of RoT, and in Fig. 6, which shows the effect of the number of subchannels. Figs. 7 and 8 study
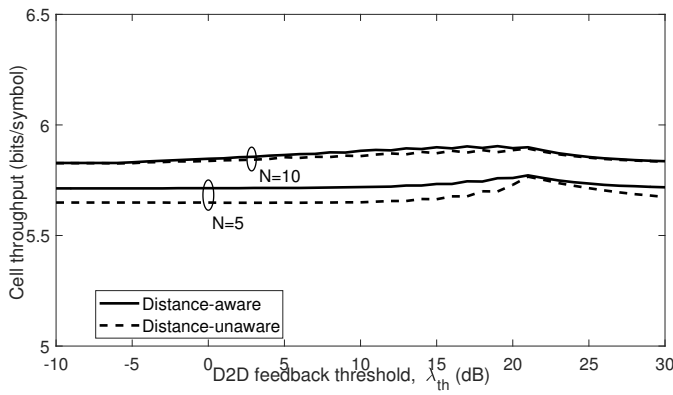
This article has been accepted for publication in a future issue of this journal, but has not been fully edited. Content may change prior to final publication. Citation information: DOI 10.1109/TWC.2017.2773616, IEEE Transactions on Wireless Communications

8

Fig. 2. Effect of λ_{th}: Zoomed-in view of cell throughput of CLISAA as a function of λ_{th} for distance-aware and distance-unaware scenarios ($M = 1$, $m = 1$, and RoT $= 0$).

the fairness and quantized direct-link CSI related extensions, respectively. Insights into mode selection as a function of D2D pair distance and the scheduler are presented in Fig. 9.

One D2D Pair ($M = 1$): Fig. 2 plots the cell throughput of CLISAA as a function of the feedback threshold λ_{th} for different number of CUs. We observe that the cell throughput at the optimal value of λ_{th} is 2.5% greater compared to that when the threshold is 0 or ∞. Also, the cell throughput of the distance-unaware scenario is relatively more sensitive to the choice of λ_{th} than that of the distance-aware scenario.

Fig. 3 benchmarks the cell throughput of CLISAA with 1-bit and 0-bit feedback for the distance-aware scenario as a function of the number of CUs N per cell. Results for CLISAA with 1-bit feedback are shown for the optimal value of λ_{th}, which is determined numerically. It turns out to be 20.9 dB, 20.6 dB, 20.6 dB, and 20.5 dB for $N = 3, 8, 13$, and 18, respectively. The cell throughputs of all the schemes increase as N increases due to multi-user diversity. With 1-bit feedback, the cell throughput of CLISAA with the optimal threshold is within 10.7% of that of complete CSI scheme over the entire range of total number of UEs considered. These results show the benefits of using direct-link and cross-link CSI statistics for rate adaptation and mode selection. Over the range of N considered, the cell throughput of CISURA is 7.8%-17.7% less than that of CLISAA with 1-bit feedback, as it ignores the cross-link interference statistics. The cell throughput of FDR is much lower for all its rates. This shows the relevance of rate adaptation in D2D even with partial CSI.

The corresponding results for the distance-unaware scenario are shown in Fig. 4. The cell throughput of CLISAA with the optimal threshold and 1-bit feedback is within 12% of that of complete CSI scheme over the entire range of total number of UEs considered. It is 7.6%-19.1% more than that of CISURA. Again, 1-bit feedback improves cell throughput compared to 0-bit feedback, but only marginally. The FDR scheme markedly underperforms CLISAA.

Two interesting observations come out of the above two figures. Firstly, CLISAA – even with 0-bit feedback – outperforms CISURA. Secondly, the cell throughput of CLISAA is insensitive to λ_{th}; this is not obvious at first sight. This is because it exploits the statistics of the cross-link interference.
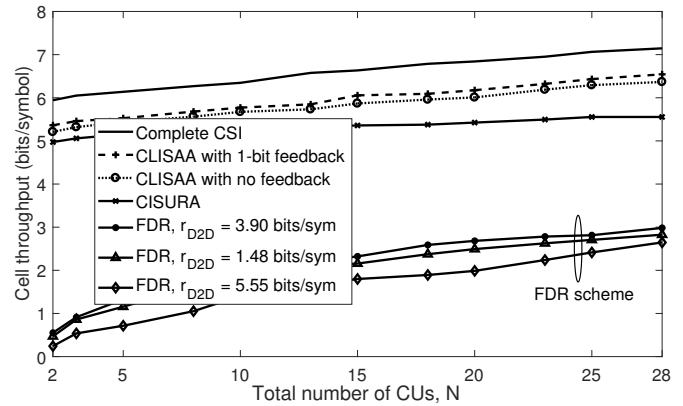

Fig. 3. Distance-aware scenario: Benchmarking of cell throughput of CLISAA with that of complete CSI, CISURA, and FDR schemes ($M = 1$, $m = 2$, and RoT $= 0$).
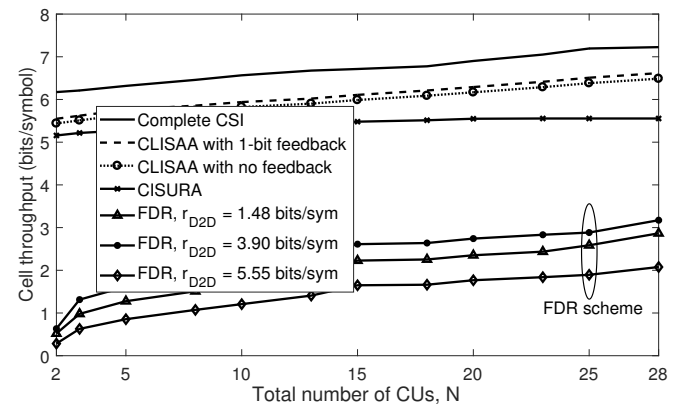

Fig. 4. Distance-unaware scenario: Benchmarking of cell throughput of CLISAA with that of complete CSI, CISURA, and FDR schemes ($M = 1$, $m = 1$, and RoT $= 0$).

Effect of ICI: Fig. 5 compares the cell throughputs of CLISAA (with 1-bit feedback), CISURA, and complete CSI scheme as a function of RoT with $U = 4$ subchannels for the distance-unaware scenario. Results for the FDR scheme are not shown to avoid clutter. CLISAA again outperforms CISURA. As expected, for all schemes, the cell throughput per subchannel increases as RoT decreases or the number of D2D pairs increases.

Multiple D2D pairs ($M \geq 1$): Fig. 6 compares the cell throughputs of CLISAA (with 1-bit feedback), CISURA, and the complete CSI scheme as a function of U with $M = 4$ and 10 D2D pairs and $N = 8$ CUs for the distance-unaware scenario.[4] Results for the FDR scheme are not shown to avoid

[4]In a cellular system with $N + 2M$ UEs, M D2D pairs can be chosen in $\prod_{k=1}^{M} \binom{N+2k}{2}$ ways, which increases exponentially in N. We, therefore, average over 500 random realizations of M D2D pairs.
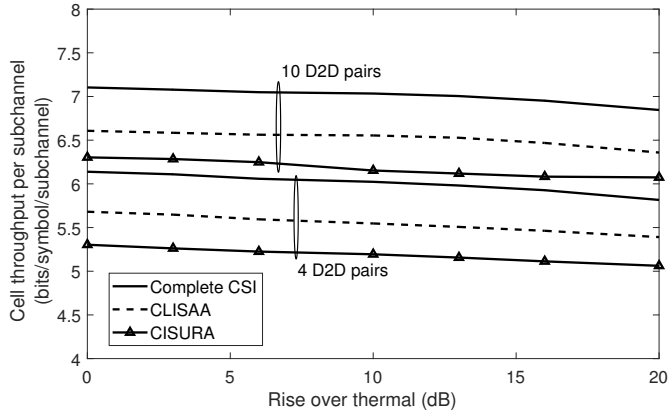
Fig. 5. Effect of RoT: Zoomed-in comparison of cell throughputs of CLISAA, CISURA, and complete CSI schemes for different numbers of D2D pairs ($N = 8$ CUs, $U = 4$ subchannels, $m = 1$, and distance-unaware scenario).
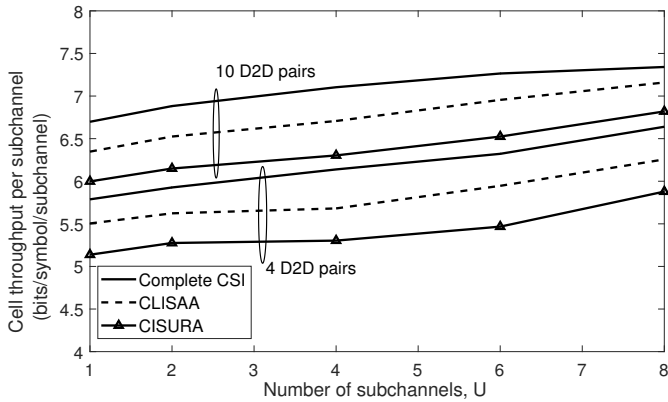

Fig. 7. PF scheduler: Benchmarking of GM of CLISAA with other schemes ($M = 1$, $m = 1$, RoT = 0, and distance-aware scenario).

Fig. 6. Multiple D2D pairs: Zoomed-in comparison of cell throughputs of CLISAA, CISURA, and complete CSI schemes for different numbers of subchannels ($N = 8$ CUs, RoT = 0, $m = 1$, and distance-unaware scenario).

clutter. As M or U increase, the cell throughput of all the schemes increases due to multi-user diversity. We again see that CLISAA outperforms CISURA.

With PF Scheduling: Now, CLISAA is used as per Result 4. For the benchmark schemes, the user scheduling and mode selection are performed to maximize the weighted rates, as in Result 4. We compare the GM of the average user throughputs in CLISAA with that of the benchmark schemes. GM helps assess the ability of a scheme to achieve the desired trade-off between average UE throughput and fairness across UEs. This is because, for a given average sum throughput, the GM is maximized when all the average user throughputs are equal [21], [22], [34]. Intuitively, the GM gives more importance to cell-edge UEs with lower throughputs, while the sum throughput is more influenced by cell-center UEs with higher throughputs.

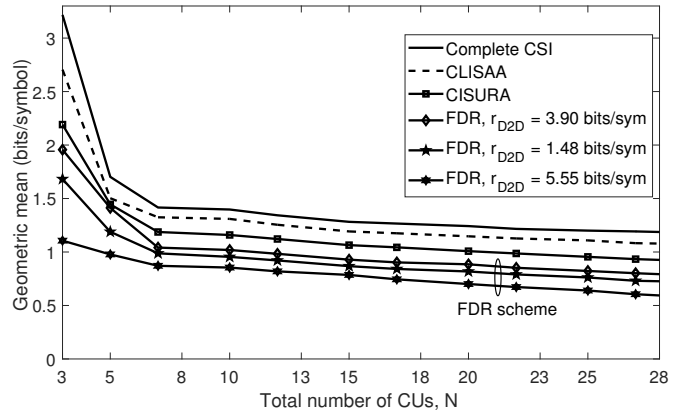Fig. 7 plots the GM of the different schemes as a function

of the number of CUs N for the distance-aware scenario. We observe that the GMs of all the schemes decrease as N increases. This is because the average throughput of each user decreases even though the sum throughput increases. Also, CLISAA achieves a higher GM than both CISURA and FDR schemes. Its GM is within 10.0%-18.9% of that of the complete CSI scheme.

With Quantized Direct-Link CSI: Fig. 8 plots the cell throughput of CLISAA with quantized CSI and 1-bit cross-link feedback for the distance-aware scenario. CISURA is modified as follows. The MCS of D2D pair j in UM is again chosen as $l_{\mathrm{DU}}^*(j, i) \approx \mathrm{argmax}_{1 \le l \le L} \left\{ r_l \mathbf{1}_{\{\Lambda_i^{\mathrm{UM}}(j) > \lambda_l\}} \right\}$, where the SINR $\Lambda_i^{\mathrm{UM}}(j)$ is a function of the index e that is fed back for the direct-link SINR and is given in Section V-A1. The FDR scheme is unchanged as it employs a fixed D2D rate. The cell throughput of CLISAA is within 12.6% of the complete CSI scheme with unquantized direct-link feedback. It is 6.6%-17.5% more than that of CISURA.

Insights about Optimal Mode Selection: Fig. 9 plots the probabilities of selection of UM, CM, and DM as a function of the distances between the DTx and DRx for the distance-unaware scenario with 10 UEs. This is done for the throughput-optimal policy and the PF scheduler. The results are presented in the form of a scatter plot that arises for the $\binom{10}{2} = 45$ possible D2D pair combinations and DTx-DRx distances. For both policies, we see that as d_j^D increases, the probability that CM is selected increases and UM is selected decreases since the D2D link becomes weaker. The probability that DM is selected is the lowest. Compared to the throughput-optimal policy, the probability that UM is selected is greater and the probability that CM is selected is smaller for the PF scheduler for a given DTx-DRx distance. This is because UM makes a CU and D2D pair transmit simultaneously and is, thus, preferable for ensuring fairness.
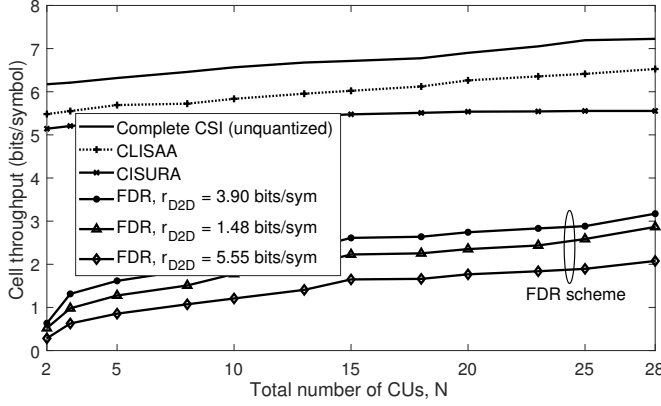
Fig. 8. Quantized direct-link SINR: Benchmarking of cell throughput of CLISAA for quantized h_j^D with complete CSI, CISURA, and FDR schemes ($M = 1$, RoT $= 0$, $m = 1$, and distance-aware scenario).
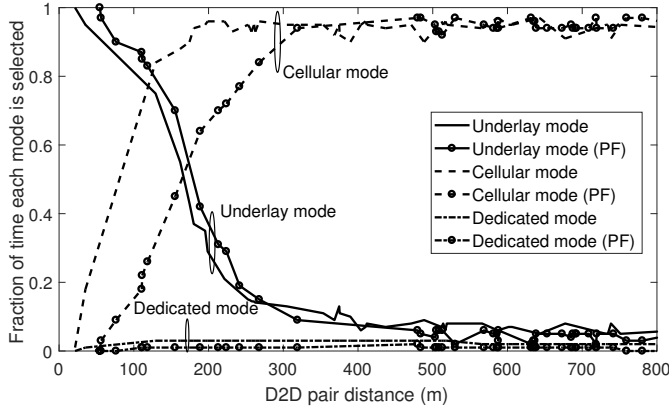

Fig. 9. Probability of selection of UM, DM, and CM as a function of D2D pair distance for cell throughput maximizing and PF scheduler based policies (10 UEs, RoT $= 0$, $M = 1$, and $m = 1$).

VI. CONCLUSIONS

We proposed a new throughput-optimal joint mode selection, user scheduling, and discrete rate adaptation policy called CLISAA for D2D systems that incorporates ICI and requires very limited feedback about the interference from the cross links that arise in it. CLISAA was also extended to address the availability of quantized direct-link CSI, ensure proportional fairness, and schedule multiple D2D pairs in a cell. Even with very limited feedback about the cross links, the cell throughput and GM of CLISAA were close to that with complete CSI at the BS. Rate adaptation was essential to achieve this and required the availability of direct-link CSI and exploitation of the statistics of the cross links. Avenues for future work with partial CSI include modeling joint rate and power adaptation, time dynamics of ICI, and multiple antennas at the BS and the UEs.

APPENDIX

A. Proof of Result 1

Let $\phi = \max\limits_{\substack{\mathbf{m},\mathbf{x}^{\mathrm{UM}},\mathbf{x}^{\mathrm{CM}},\mathbf{z}^D(j,i),\\ \mathbf{z}^C(i,j),\mathbf{z}^{\mathrm{CM}}(i),\mathbf{z}^{\mathrm{DM}}(j)}} \left\{ \mathbb{E}_{q_{ij}}\left[T|\mathbf{g}_B^C, g_{j,B}^D, h_j^D, \mathbf{f}_b(j)\right]\right\}$, where T is given in (6). Since only the D2D pair SINR $\Gamma_i^{\mathrm{UM}}(j)$ in UM is a function of q_{ij}, due to the additive form of T, the above conditional expectation simplifies to

$$\phi = \max\limits_{\substack{\mathbf{m},\mathbf{x}^{\mathrm{UM}},\mathbf{x}^{\mathrm{CM}},\mathbf{z}^D(j,i),\\ \mathbf{z}^C(i,j),\mathbf{z}^{\mathrm{CM}}(i),\mathbf{z}^{\mathrm{DM}}(j)}} \left\{ m_1 \right.$$
$$\times \left[\sum_{i=1}^{N} x_i^{\mathrm{UM}}\left(\sum_{l=1}^{L} z_l^C(i,j)r_l 1_{\{\gamma_j^{\mathrm{UM}}(i)\geq\lambda_l\}} \right.\right.$$
$$\left.\left. + \sum_{l=1}^{L} z_l^D(j,i)\, r_l \Pr\left(\Gamma_i^{\mathrm{UM}}(j) > \lambda_l | \mathbf{f}_b(j), \mathbf{g}_B^C, g_{j,B}^D, h_j^D\right) \right) \right]$$
$$+ m_2 \left[\sum_{i=1}^{N} x_i^{\mathrm{CM}} \sum_{l=1}^{L} z_l^{\mathrm{CM}}(i)r_l 1_{\{\gamma^{\mathrm{CM}}(i)\geq\lambda_l\}} \right]$$
$$+ m_3 \left.\left[\sum_{l=1}^{L} z_l^{\mathrm{DM}}(j)r_l 1_{\{\Gamma^{\mathrm{DM}}(j)\geq\lambda_l\}} \right]\right\}. \quad (31)$$

The maximization in (31) can be written in terms of a cascade of individual maximizations over $\mathbf{m}, \mathbf{x}^{\mathrm{UM}}, \mathbf{x}^{\mathrm{CM}}, \mathbf{z}^D(j,i), \mathbf{z}^C(i,j), \mathbf{z}^{\mathrm{CM}}(i)$, and $\mathbf{z}^{\mathrm{DM}}(j)$ based on the following observations:

1) The CU MCS selection in UM depends only on $\gamma_j^{\mathrm{UM}}(i)$. Therefore, maximization over $\mathbf{z}^D(j,i)$, $\mathbf{z}^{\mathrm{CM}}(i)$, and $\mathbf{z}^{\mathrm{DM}}(j)$ is not needed in the first term, which is given by $x_i^{\mathrm{UM}} \sum_{l=1}^{L} z_l^C(i,j)r_l 1_{\{\gamma_j^{\mathrm{UM}}(i)\geq\lambda_l\}}$.

2) In the second term $x_i^{\mathrm{UM}} \sum_{l=1}^{L} z_l^D(j,i)\, r_l \times \Pr\left(\Gamma_i^{\mathrm{UM}}(j) > \lambda_l | \mathbf{f}_b(j), \mathbf{g}_B^C, g_{j,B}^D, h_j^D\right)$, the selection of the MCS of the D2D users in UM depends on $\Gamma_i^{\mathrm{UM}}(j)$, and the maximization over $\mathbf{z}^C(i,j)$, $\mathbf{z}^{\mathrm{CM}}(i)$, and $\mathbf{z}^{\mathrm{DM}}(j)$ is not needed. Also, the above two terms do not depend on $\mathbf{x}^{\mathrm{CM}}$.

3) For selecting the MCS of a CU in CM in the third term $x_i^{\mathrm{CM}} \sum_{l=1}^{L} z_l^{\mathrm{CM}}(i)r_l 1_{\{\gamma^{\mathrm{CM}}(i)\geq\lambda_l\}}$, the maximization over $\mathbf{z}^D(j,i)$, $\mathbf{z}^C(i,j)$, and $\mathbf{z}^{\mathrm{DM}}(j)$ is not needed. Furthermore, this term does not depend on $\mathbf{x}^{\mathrm{UM}}$.

4) Similarly, for the MCS selection of a DU in DM in the fourth term $\sum_{l=1}^{L} z_l^{\mathrm{DM}}(j)r_l 1_{\{\Gamma^{\mathrm{DM}}(j)\geq\lambda_l\}}$, the maximization over $\mathbf{z}^D(j,i)$, $\mathbf{z}^C(i,j)$, and $\mathbf{z}^{\mathrm{CM}}(i)$ is not needed. Furthermore, this term does not depend on $\mathbf{x}^{\mathrm{UM}}$ and $\mathbf{x}^{\mathrm{CM}}$.

Therefore, by retaining the maximization pertinent to each

term, ϕ simplifies to

$$\phi =$$

$$\max_{\mathbf{m}} \left\{ m_1 \max_{\mathbf{x}^{\text{UM}}} \left\{ \sum_{i=1}^{N} x_i^{\text{UM}} \max_{\mathbf{z}^C(i,j)} \left\{ \sum_{l=1}^{L} z_l^C(i,j) r_l 1_{\{\gamma_j^{\text{UM}}(i) \geq \lambda_l\}} \right\} \right. \right.$$

$$+ \max_{\mathbf{z}^D(j,i)} \left\{ \sum_{l=1}^{L} z_l^D(j,i)\, r_l \Pr\big(\Gamma_i^{\text{UM}}(j) > \lambda_l | \mathbf{f}_b(j), \mathbf{g}_B^C, g_{j,B}^D, h_j^D\big) \right\} \right\}$$

$$+ m_2 \max_{\mathbf{x}^{\text{CM}}} \left\{ \sum_{i=1}^{N} x_i^{\text{CM}} \max_{\mathbf{z}^{\text{CM}}(i)} \left\{ \sum_{l=1}^{L} z_l^{\text{CM}}(i) r_l 1_{\{\gamma^{\text{CM}}(i) \geq \lambda_l\}} \right\} \right\}$$

$$\left. + m_3 \sum_{l=1}^{L} \max_{\mathbf{z}^{\text{DM}}(j)} \left\{ z_l^{\text{DM}}(j) r_l 1_{\{\Gamma^{\text{DM}}(j) \geq \lambda_l\}} \right\} \right\}. \tag{32}$$

From (32), to maximize $\sum_{l=1}^{L} z_l^C(i,j) r_l 1_{\{\gamma_j^{\text{UM}}(i) \geq \lambda_l\}}$ subject to the constraint that $\sum_{l=1}^{L} z_l^C(i,j) = 1$ and $z_1^C(i,j), z_2^C(i,j), \ldots, z_L^C(i,j)$ are binary variables, it follows that $z_l^C(i,j)$ should be 1 for the MCS l that maximizes $r_l 1_{\{\gamma_j^{\text{UM}}(i) \geq \lambda_l\}}$, and is 0 for all other MCSs. This yields the result in (11) for $l_{\text{CU}}^*(i,j)$. Next, to maximize $\sum_{l=1}^{L} z_l^D(j,i) r_l \Pr\big(\Gamma_i^{\text{UM}}(j) > \lambda_l | \mathbf{f}_b(j), \mathbf{g}_B^C, g_{j,B}^D, h_j^D\big)$ subject to the constraint $\sum_{l=1}^{L} z_l^D(j,i) = 1$ and $z_1^D(j,i), \ldots, z_L^D(j,i)$ are binary variables, it follows that $z_l^D(j,i)$ is 1 for the MCS l that maximizes $r_l \Pr\big(\Gamma_i^{\text{UM}}(j) > \lambda_l | \mathbf{f}_b(j), \mathbf{g}_B^C, g_{j,B}^D, h_j^D\big)$ and is 0 for all other MCSs. This yields the result in (10) for $l_{\text{DU}}^*(j,i)$. Similarly, $z_l^{\text{CM}}(i)$ should be 1 for the MCS l that maximizes $r_l 1_{\{\gamma^{\text{CM}}(i) \geq \lambda_l\}}$ and is 0 otherwise, which yields the result in (12) for $l_{\text{CM}}^*(i)$. And, $z_l^{\text{DM}}(j)$ should be 1 for the MCS l that maximizes $r_l 1_{\{\Gamma^{\text{DM}}(j) \geq \lambda_l\}}$ and is 0 otherwise, which yields the result in (13) for $l_{\text{DM}}^*(j)$.

Hence, (32) simplifies to

$$\phi = \max_{\mathbf{m}} \left\{ m_1 \max_{\mathbf{x}^{\text{UM}}} \left\{ \sum_{i=1}^{N} x_i^{\text{UM}} \left(r_{l_{\text{CU}}^*(i,j)} + r_{l_{\text{DU}}^*(j,i)} \right) \right\} \right.$$

$$\left. + m_2 \max_{\mathbf{x}^{\text{CM}}} \left\{ \sum_{i=1}^{N} x_i^{\text{CM}} r_{l_{\text{CM}}^*(i)} \right\} + m_3 r_{l_{\text{DM}}^*(j)} \right\}. \tag{33}$$

In (33), to maximize the sum $\sum_{i=1}^{N} x_i^{\text{UM}} (r_{l_{\text{CU}}^*(i,j)} + r_{l_{\text{DU}}^*(j,i)})$ subject to the constraints $\sum_{i=1}^{N} x_i^{\text{CM}} = 1$ and $x_1^{\text{UM}}, x_2^{\text{UM}}, \ldots, x_N^{\text{UM}}$ are binary variables, it follows that x_i^{UM} should be 1 for the CU i that maximizes $r_{l_{\text{CU}}^*(i,j)} + r_{l_{\text{DU}}^*(j,i)}$, and is 0 for all other CUs. This yields (14) for i_{UM}^*. Similarly, x_i^{CM} should be 1 for the CU i that maximizes $r_{l_{\text{CM}}^*(i)}$ and is 0 otherwise. This yields (15) for i_{CM}^*.

Thus, (33) simplifies to

$$\phi = \max_{\mathbf{m}} \left\{ m_1 \tau_{\text{UM}} + m_2 \tau_{\text{CM}} + m_3 \tau_{\text{DM}} \right\}, \tag{34}$$

where $\tau_{\text{UM}} = r_{l_{\text{CU}}^*(i_{\text{UM}}^*,j)} + r_{l_{\text{DU}}^*(j,i_{\text{UM}}^*)}$, $\tau_{\text{CM}} = r_{l_{\text{CM}}^*(i_{\text{CM}}^*)}$, and $\tau_{\text{DM}} = r_{l_{\text{DM}}^*(j)}$. Again, maximizing ϕ subject to the constraint $\sum_{v=1}^{3} m_v = 1$ and m_1, m_2, and m_3 are binary variables, yields the final result in (16).

B. Proof of Result 2

From (2), $\Pr\big(\Gamma_i^{\text{UM}}(j) > \lambda_l | \mathbf{f}_b(j), \mathbf{g}_B^C, g_{j,B}^D, h_j^D\big)$ does not depend on $\mathbf{g}_B^C$, $g_{j,B}^D$, and $f_b(k,j)$, for $k \neq i$. We consider the cases $f_b(i,j) = 1$ and $f_b(i,j) = 0$ separately below.

1. When $f_b(i,j) = 1$: In this case, $\Gamma_i^{\text{UM}}(j) \geq \lambda_{\text{th}}$. In UM, the feedback-conditioned goodput is $r_l P_1(l)$, where $P_1(l) = \Pr\big(\Gamma_i^{\text{UM}}(j) > \lambda_l | \Gamma_i^{\text{UM}}(j) \geq \lambda_{\text{th}}, \mathbf{g}_B^C, g_{j,B}^D, h_j^D, d_{ij}\big)$. Substituting the expression for $\Gamma_i^{\text{UM}}(j)$ from (2), rearranging terms, and using Bayes' theorem, we get

$$P_1(l) =$$

$$\frac{\Pr\left(q_{ij} < \frac{P_D h_j^D - (1+\text{RoT})\sigma^2 \max\{\lambda_l, \lambda_{\text{th}}\}}{P_C \max\{\lambda_l, \lambda_{\text{th}}\}} | \mathbf{g}_B^C, g_{j,B}^D, h_j^D, d_{ij} \right)}{\Pr\left(q_{ij} < \frac{P_D h_j^D - (1+\text{RoT})\sigma^2 \lambda_{\text{th}}}{P_C \lambda_{\text{th}}} | \mathbf{g}_B^C, g_{j,B}^D, h_j^D, d_{ij} \right)}. \tag{35}$$

Upon substituting the CDF of q_{ij}, which is a Nakagami-m RV, and simplifying further yields the result in (17) corresponding to $f_b(i,j) = 1$.

2. When $f_b(i,j) = 0$: In this case, we are given that $\Gamma_i^{\text{UM}}(j) < \lambda_{\text{th}}$. The feedback-conditioned goodput is $r_l P_0(l)$, where $P_0(l) = \Pr\big(\Gamma_i^{\text{UM}}(j) > \lambda_l | \Gamma_i^{\text{UM}}(j) < \lambda_{\text{th}}, \mathbf{g}_B^C, g_{j,B}^D, h_j^D, d_{ij}\big)$. Using Bayes' theorem, we get

$$P_0(l) = 1 - \frac{\Pr\big(\Gamma_i^{\text{UM}}(j) < \min\{\lambda_l, \lambda_{\text{th}}\} | \mathbf{g}_B^C, g_{j,B}^D, h_j^D, d_{ij}\big)}{\Pr\big(\Gamma_i^{\text{UM}}(j) < \lambda_{\text{th}} | \mathbf{g}_B^C, g_{j,B}^D, h_j^D, d_{ij}\big)}. \tag{36}$$

Substituting the expression for $\Gamma_i^{\text{UM}}(j)$ and rearranging terms,

$$P_0(l) = 1$$

$$- \frac{\Pr\left(q_{ij} > \frac{P_D h_j^D - (1+\text{RoT})\sigma^2 \min\{\lambda_l, \lambda_{\text{th}}\}}{P_C \min\{\lambda_l, \lambda_{\text{th}}\}} | \mathbf{g}_B^C, g_{j,B}^D, h_j^D, d_{ij} \right)}{\Pr\left(q_{ij} > \frac{P_D h_j^D - (1+\text{RoT})\sigma^2 \lambda_{\text{th}}}{P_C \lambda_{\text{th}}} | \mathbf{g}_B^C, g_{j,B}^D, h_j^D, d_{ij} \right)}. \tag{37}$$

Simplifying further yields the result in (17) that corresponds to $f_b(i,j) = 0$.

C. Proof of Lemma 1

Without loss of generality, let the BS, DRx, and CU be located at $(0,0)$, (x, y), and $(s, 0)$, respectively. Let C_1 denote a circular area with center $(0,0)$ and radius R; it corresponds to the set of all DRx locations. Let C_2 denote a circular area of radius R and the CU as its center.

Consider the following transformation from C_1 to C_2, which is shown in Fig. 10. If a point $p = (x, y) \in C_1 \cap C_2^c$, then it is mapped to the point $p' = (s - x, y)$. Else, if $p \in C_1 \cap C_2$, then p is mapped to itself. It is easy to verify that the transformation is bijective.

1) *When $p = (x, y) \in C_1 \cap C_2^c$:* Its distance from the CU is $\sqrt{(x-s)^2 + y^2}$. Since $p \in C_1 \cap C_2^c$, it is easy to prove that $x \leq s/2$. The distance between p'' and the CU is $\sqrt{x^2 + y^2}$. This implies that $p'' \in C_2$ since $\sqrt{x^2 + y^2} \leq R$. Furthermore, since $x \leq s/2$, it follows that $\sqrt{x^2 + y^2} \leq \sqrt{(x-s)^2 + y^2}$.

This article has been accepted for publication in a future issue of this journal, but has not been fully edited. Content may change prior to final publication. Citation information: DOI 10.1109/TWC.2017.2773616, IEEE Transactions on Wireless Communications
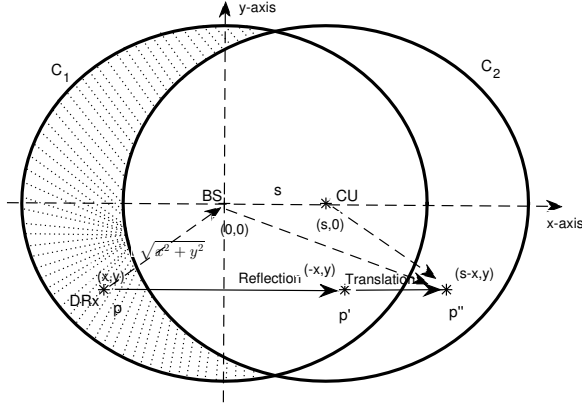
12

Fig. 10. Illustration of bijective transformation from points in the circle with BS at the center to points in the circle with the CU at the center.

2) *When $p = (x, y) \in C_1 \cap C_2$:* In this case, the distance to the CU remains unchanged.

Thus, the distance between a mapped point in C_2 and the CU is always less than or equal to that between its corresponding point in C_1 and the CU. Hence, the result follows.

D. Proof of Result 3

As before, we consider the two cases $f_b(i, j) = 1$ and $f_b(i, j) = 0$ separately below.

1) When $f_b(i, j) = 1$: As in Appendix B, the feedback-conditioned goodput is $r_l \psi_1(l)$, where $\psi_1(l) = \mathbb{E}_{d_{ij}}[P_1(l)]$. Substituting the CDF of q_{ij}, which is an exponential RV, in (35), we get

$$\psi_1(l) = \mathbb{E}_{d_{ij}} \left[\frac{1 - \exp\left(-\frac{[P_D h_j^D - (1+\text{RoT})\sigma^2 \max\{\lambda_l, \lambda_{\text{th}}\}]^+}{P_C K d_{ij}^{-\alpha} \max\{\lambda_l, \lambda_{\text{th}}\}}\right)}{1 - \exp\left(-\frac{[P_D h_j^D - (1+\text{RoT})\sigma^2 \lambda_{\text{th}}]^+}{P_C K d_{ij}^{-\alpha} \lambda_{\text{th}}}\right)} \right]. \quad (38)$$

In order to ensure tractability, we drop $[.]^+$, which is a tight approximation since $P_D h_j^D / \sigma^2 > \lambda_l$ with high probability except for cell-edge UEs, and average over d'_{ij} as per Lemma 1. This yields

$$\psi_1(l) \approx \mathbb{E}_{d'_{ij}} \left[\frac{1 - \exp\left(-\frac{P_D h_j^D - (1+\text{RoT})\sigma^2 \max\{\lambda_l, \lambda_{\text{th}}\}}{P_C K (d'_{ij})^{-\alpha} \max\{\lambda_l, \lambda_{\text{th}}\}}\right)}{1 - \exp\left(-\frac{P_D h_j^D - (1+\text{RoT})\sigma^2 \lambda_{\text{th}}}{P_C K (d'_{ij})^{-\alpha} \lambda_{\text{th}}}\right)} \right]. \quad (39)$$

Using the binomial expansion for the denominator in (39), we get

$$\psi_1(l) =$$
$$\mathbb{E}_{d'_{ij}} \left[\left[1 - \exp\left(-\frac{P_D h_j^D - (1+\text{RoT})\sigma^2 \max\{\lambda_l, \lambda_{\text{th}}\}}{P_C K (d'_{ij})^{-\alpha} \max\{\lambda_l, \lambda_{\text{th}}\}}\right) \right] \right.$$
$$\left. \times \sum_{n=0}^{\infty} \exp\left(-\frac{P_D h_j^D - (1+\text{RoT})\sigma^2 \lambda_{\text{th}}}{P_C K (d'_{ij})^{-\alpha} \lambda_{\text{th}}} n\right) \right]. \quad (40)$$

Interchanging the order of expectation and infinite summation, which is justified by the dominated convergence theorem (DCT), and simplifying yields (18).

2) When $f_b(i, j) = 0$: For this case, the feedback-conditioned goodput is $r_l \psi_0(l)$, where $\psi_0(l) = \mathbb{E}_{d_{ij}}[P_0(l)]$. Substituting the CDF of q_{ij} in (37), we get

$$\psi_0(l) = 1 -$$
$$\mathbb{E}_{d_{ij}} \left[\exp\left(-\frac{[P_D h_j^D - (1+\text{RoT})\sigma^2 \min\{\lambda_l, \lambda_{\text{th}}\}]^+}{P_C K d_{ij}^{-\alpha} \min\{\lambda_l, \lambda_{\text{th}}\}} \right. \right.$$
$$\left. \left. + \frac{[P_D h_j^D - (1+\text{RoT})\sigma^2 \lambda_l]^+}{P_C K d_{ij}^{-\alpha} \lambda_l} \right) \right]. \quad (41)$$

As before, removing $(\cdot)^+$, using Lemma 1, and simplifying, we get

$$\psi_0(l) \approx 1 -$$
$$\mathbb{E}_{d'_{ij}} \left[\exp\left(-\frac{P_D h_j^D - (1+\text{RoT})\sigma^2 \min\{\lambda_l, \lambda_{\text{th}}\}}{P_C K (d'_{ij})^{-\alpha} \min\{\lambda_l, \lambda_{\text{th}}\}} \right. \right.$$
$$\left. \left. + \frac{P_D h_j^D - (1+\text{RoT})\sigma^2 \lambda_l}{P_C K (d'_{ij})^{-\alpha} \lambda_l} \right) \right]. \quad (42)$$

Evaluating this expectation and simplifying it yields (19).

REFERENCES

[1] H. Min, J. Lee, S. Park, and D. Hong, "Capacity enhancement using an interference limited area for device-to-device uplink underlaying cellular networks," *IEEE Trans. Wireless Commun.*, vol. 10, no. 12, pp. 3995–4000, Dec. 2011.

[2] D. Feng, L. Lu, Y. Yuan-Wu, G. Li, G. Feng, and S. Li, "Device-to-device communications underlaying cellular networks," *IEEE Trans. Commun*, vol. 61, no. 8, pp. 3541–3551, Aug. 2013.

[3] G. Yu, L. Xu, D. Feng, R. Yin, G. Li, and Y. Jiang, "Joint mode selection and resource allocation for device-to-device communications," *IEEE Trans. Commun*, vol. 62, no. 11, pp. 3814–3824, Nov. 2014.

[4] P. Janis, V. Koivunen, C. Ribeiro, J. Korhonen, K. Doppler, and K. Hugl, "Interference-aware resource allocation for device-to-device radio underlaying cellular networks," in *Proc. VTC (Spring)*, Apr. 2009, pp. 1–5.

[5] C.-H. Yu, O. Tirkkonen, K. Doppler, and C. Ribeiro, "On the performance of device-to-device underlay communication with simple power control," in *Proc. VTC (Spring)*, Apr. 2009, pp. 1–5.

[6] C.-H. Yu, K. Doppler, C. Ribeiro, and O. Tirkkonen, "Resource sharing optimization for device-to-device communication underlaying cellular networks," *IEEE Trans. Wireless Commun.*, vol. 10, no. 8, pp. 2752–2763, Aug. 2011.

[7] K. Doppler, C.-H. Yu, C. Ribeiro, and P. Janis, "Mode selection for device-to-device communication underlaying an LTE-advanced network," in *Proc. WCNC*, Apr. 2010, pp. 1–6.

[8] Z. Liu, T. Peng, S. Xiang, and W. Wang, "Mode selection for device-to-device (D2D) communication under LTE-advanced networks," in *Proc. ICC*, Jun. 2012, pp. 5563–5567.

[9] N. Lee, X. Lin, J. G. Andrews, and R. W. Heath, "Power control for D2D underlaid cellular networks: Modeling, algorithms, and analysis," *IEEE J. Sel. Areas Commun.*, vol. 33, no. 1, pp. 1–13, Jan. 2015.

[10] D. Wu, J. Cai, J. Qi, and J. J. P. C. Rodrigues, "Uplink dynamic resource sharing of underlaying D2D and cellular communications," in *Proc. WCSP*, Oct. 2014, pp. 1–6.

[11] H. H. Esmat, M. M. Elmesalawy, and I. I. Ibrahim, "Adaptive resource sharing algorithm for device-to-device communications underlaying cellular networks," *IEEE Commun. Lett.*, vol. 20, no. 3, pp. 530–533, Mar. 2016.

[12] R. Gupta, S. Kalyanasundaram, and P. R. A. Kumar, "Transmission mode selection and resource allocation for D2D unicast communications," in *Proc. VTC (Fall)*, Sep. 2016, pp. 1–7.

[13] X. Lin, R. W. Heath, and J. G. Andrews, "The interplay between massive MIMO and underlaid D2D networking," *IEEE Trans. Wireless Commun.*, vol. 14, no. 6, pp. 3337–3351, Jun. 2015.

[14] L. B. Le, "Fair resource allocation for device-to-device communications in wireless cellular networks," in *Proc. Globecom*, Dec. 2012, pp. 5451–5456.

[15] Y. S. Liou, R. H. Gau, and C. J. Chang, "Group partition and dynamic rate adaptation for scalable capacity-region-aware device-to-device communications," *IEEE Trans. Wireless Commun.*, vol. 14, no. 2, pp. 921–934, Feb. 2015.

[16] S. Sesia, I. Toufik, and M. Baker, *LTE, The UMTS Long Term Evolution: From Theory to Practice*. Wiley, 2009.

[17] Y. J. Choi and S. Rangarajan, "Analysis of best channel feedback and its adaptive algorithms for multicarrier wireless data systems," *IEEE Trans. Mob. Comput.*, vol. 10, no. 8, pp. 1071–1082, Aug. 2011.

[18] J. Leinonen, J. Hämäläinen, and M. Juntti, "Performance analysis of downlink OFDMA resource allocation with limited feedback," *IEEE Trans. Wireless Commun.*, vol. 8, no. 6, pp. 2927–2937, Jun. 2009.

[19] S. Sanayei and A. Nosratinia, "Opportunistic downlink transmission with limited feedback," *IEEE Trans. Inf. Theory*, vol. 53, no. 11, pp. 4363–4372, Nov. 2007.

[20] V. Hassel, D. Gesbert, M.-S. Alouini, and G. E. Øien, "A threshold-based channel state feedback algorithm for modern cellular systems," *IEEE Trans. Wireless Commun.*, vol. 6, no. 7, pp. 2422–2426, Jul. 2007.

[21] R. Fritzsche, P. Rost, and G. P. Fettweis, "Robust rate adaptation and proportional fair scheduling with imperfect CSI," *IEEE Trans. Wireless Commun.*, vol. 14, no. 8, pp. 4417–4427, Aug. 2015.

[22] S. Gulati, S. Kalyanasundaram, P. Nashine, B. Natarajan, R. Agrawal, and A. Bedekar, "Performance analysis of distributed multi-cell coordinated scheduler," in *Proc. VTC (Fall)*, Sep. 2015, pp. 1–5.

[23] S. Shalmashi, G. Miao, and S. B. Slimane, "Interference management for multiple device-to-device communications underlaying cellular networks," in *Proc. PIMRC*, Sept. 2013, pp. 223–227.

[24] D. Feng, L. Lu, Y.-W. Yi, G. Y. Li, G. Feng, and S. Li, "QoS-aware resource allocation for device-to-device communications with channel uncertainty," *IEEE Trans. Veh. Technol.*, vol. 65, no. 8, pp. 6051–6062, Aug. 2016.

[25] R. Wang, J. Zhang, S. H. Song, and K. B. Letaief, "Optimal QoS-aware channel assignment in D2D communications with partial CSI," *IEEE Trans. Wireless Commun.*, vol. 15, no. 11, pp. 7594–7609, Nov. 2016.

[26] H. Tang and Z. Ding, "Monotonic optimization for power control of D2D underlay with partial CSI," in *Proc. ICC*, May 2016, pp. 1–6.

[27] M. Mozaffari, W. Saad, M. Bennis, and M. Debbah, "Unmanned aerial vehicle with underlaid device-to-device communications: Performance and tradeoffs," *IEEE Trans. Wireless Commun.*, vol. 15, no. 6, pp. 3949–3963, Jun. 2016.

[28] J. Gu, S. J. Bae, S. F. Hasan, and M. Y. Chung, "Heuristic algorithm for proportional fair scheduling in D2D-cellular systems," *IEEE Trans. Wireless Commun.*, vol. 15, no. 1, pp. 769–780, Jan. 2016.

[29] M. Abramowitz and I. Stegun, *Handbook of Mathematical Functions, With Formulas, Graphs, and Mathematical Tables*. Dover, 1974.

[30] A. Goldsmith, *Wireless Communications*. Cambridge Univ. Press, 2005.

[31] K. L. Baum, T. A. Kostas, P. J. Sartori, and B. K. Classon, "Performance characteristics of cellular systems with different link adaptation strategies," *IEEE Trans. Veh. Technol.*, vol. 52, no. 6, pp. 1497–1507, Nov. 2003.

[32] H. Holma and A. Toskala, *WCDMA for UMTS: Radio Access for Third Generation Mobile Communications*, 1ˢᵗ ed. New York, NY, USA: John Wiley & Sons, Inc., 2000.

[33] D. Moltchanov, "Survey paper: Distance distributions in random networks," *Ad Hoc Netw.*, vol. 10, no. 6, pp. 1146–1166, Aug. 2012.

[34] R. Fritzsche, P. Rost, and G. P. Fettweis, "Opportunistic beamforming using dumb antennas," *IEEE Trans. Inf. Theory*, vol. 48, no. 6, pp. 1277–1294, Jun. 2002.

Saikiran Bulusu (S'16) received his Bachelor of Technology degree in Electronics and Communications Engineering from Mahatma Gandhi Institute of Technology, Hyderabad in 2009 and his Master of Technology degree in Communication Engineering from the Indian Institute of Technology (IIT), Madras in 2012. He worked in the Department of Electrical Communication Engineering, Indian Institute of Science (IISc), Bangalore as a Project Associate. He is now pursuing his Ph.D. in the Department of Electrical and Computer Science, Syracuse University (SU), Syracuse. His research interests include the design and performance analysis of partial feedback schemes for rate adaptation and resource allocation in D2D systems.

Neelesh B. Mehta (S'98-M'01-SM'06) received his Bachelor of Technology degree in Electronics and Communications Engineering from the Indian Institute of Technology (IIT), Madras in 1996, and his M.S. and Ph.D. degrees in Electrical Engineering from the California Institute of Technology, Pasadena, USA in 1997 and 2001, respectively. He is a Professor in the Department of Electrical Communication Engineering, Indian Institute of Science, Bangalore. He is a Fellow of the Indian National Academy of Engineering (INAE) and the National Academy of Sciences India (NASI). He is a recipient of the Shanti Swarup Bhatnagar Award 2017 and the Swarnjayanti Fellowship. He serves as the Chair of the Executive Editorial Committee of the IEEE Transactions on Wireless Communications, and as an Editor of the IEEE Transactions on Communications. He served on the Board of Governors of IEEE ComSoc from 2012 to 2015.

Suresh Kalyanasundaram is a Distinguished Member of the Technical Staff at Nokia. He obtained his B.E. (Hons.) in Electrical and Electronics Engineering, and M. Sc. (Hons.) Physics from the Birla Institute of Technology and Science, Pilani, India in 1996, and his Ph. D. degree in Electrical Engineering from Purdue University in 2000. Since then he has worked in Motorola and Nokia Networks. He was inducted as an associate member of the Motorola Science Advisory Board (SABA) in 2007. His research interests are in the area of performance analysis and radio resource management algorithms for wireless cellular networks.